L. CHEN, S.S. WANG, F. Y. ZHU, W. Z. YAN, H. C. JI

ISSN 0543-5846
METABK 63(3-4) 447-450 (2024)
UDC – UDK 669.15:621.876:621.886.4:518.1:620.16-539.374=111

ANALYSIS OF THE FORCE ON THE BALANCE BEAM OF THE LIFTING DEVICE

Received – Primljeno: 2024-02-10
Accepted – Prihvaćeno: 2024-04-10
Original Scientific Paper – Izvorni znanstveni rad

In the process of hoisting the memorial archway, because the balance beam directly lifts the memorial archway, it is easy to deform during the hoisting process, and the deformation will affect the follow-up work, resulting in the delay of the project progress. In order to avoid this situation, the existing conditions are used to calculate the load that the balance beam can bear. Using 3D modeling and numerical simulation software, conduct force analysis on the balanced beam, and compare the simulation results with the calculated values to determine whether the stress and deformation of the balanced beam meet the requirements. The simulation results show that the stress on the balance beam during the lifting process does not exceed the maximum yield stress of its own material, which meets the requirements of the working conditions.

Keywords: steel Q235B; lifting; balance beam; numerical simulation; stress-strain

INTRODUCTION

Hoisting is a construction job that uses lifting equipment to lift components and install them fixed in the design position. It is divided into separate lifting and overall lifting. The former involves sequentially hoisting the various components of buildings and structures; The latter involves assembling various components into a complete structure on the ground and then lifting them. This time, the former is used, which lifts different types of balance beams in order to the designated position. Mehran Ghafouri et al. developed a thermal metallurgical mechanical finite element (FE) model that combines the solid-state phase transition (SSPT) effect to accurately simulate the deformation of ultra-high strength carbon steel single bead plate welding. The modeling of heat source and thermal boundary conditions was completed in the ABAQUS sub program. From the results of mechanical simulation (with and without considering the influence of SSPT) and comparison with the measured deformation, it can be observed that when the influence of SSPT is included in the studied material, the angle and bending deformation caused by welding can be more accurately predicted [1]. Jorge Bonilla et al. aim to better understand the behavior of bent steel plate beams in order to develop appropriate design methods to consider the specific responses of these structures. A comprehensive numerical study was conducted on curved I-beams, taking into account material and geometric nonlinearity as well as initial defects. The numerical model was validated through experimental testing using ABAQUS software. The numerical results indicate that the elastic critical buckling load increases with the increase of span to plane radius, and can be conservatively estimated using the provisions of EN1993-1-5 for straight steel beams, and the ultimate repair loading resistance decreases with the increase of curvature radius [2]. Xu Qing and others conducted cyclic load tests on thin-walled concrete filled steel tube (CFST) bridge piers to study their ultimate seismic performance. A three-dimensional solid shell finite element (FE) model of thin-walled CFST bridge piers was established using ABAQUS. The finite element model was validated through load testing. Analysis shows that under the same intensity of seismic waves, the seismic response of fully filled thin-walled CFST bridge piers is the smallest, and filling with concrete can improve the ultimate seismic capacity [3]. Zhao Hui and others conducted experimental and numerical studies on the impact and post impact behavior of H-shaped steel components. Establish a finite element model using ABAQUS software. The explicit and implicit algorithms in ABAQUS were used to reproduce the impact test and the axial compression test after impact, respectively. To evaluate the residual bearing capacity of H-shaped steel components damaged by impact in industrial buildings. The results indicate that boundary conditions have an impact on the failure mode and impact force response during the impact process; Within the range of working parameters, the residual bearing capacity of H-shaped steel members is mainly affected by the global deformation at the mid to high

L. Chen, H. C. Ji (E-mail: jihongchao@ncst.edu.cn) College of Mechanical Engineering, North China University of Science and Technology, Hebei, Tangshan, China. S.S. Wang, F. Y. Zhu, W. Z. Yan, China MCC 22 group Corporation Limited. This work is supported by China Minmetals Group Co., Ltd. Science and Technology Special Plan Project (2021ZXA06).

altitude caused by impact [4]. Qi Lu et al. used Abaqus/Explicit to construct a finite element numerical model, verified the accuracy of the model, and conducted a series of studies. The mechanical properties of NPH at different angles under different loading conditions were analyzed, and the results showed that NPH-120 and NPH-105 had the best mechanical properties under loading conditions in the y and x directions, respectively. Subsequently, the mechanical properties of NPH were studied at different speeds. Research has shown that the NPR effect of NPH is most pronounced under low-speed impact, and the inertia effect increases with the increase of speed [5].

This article uses Q235 steel as the balance beam material in engineering, establishes a model for finite element simulation, and analyzes the force and deformation of the balance beam during actual lifting operation.

FINITE ELEMENT MODEL ESTABLISHMENT

Q235 is a low-carbon steel with good plasticity and welding performance, and good forming ability. Many profiles (such as angle steel, round steel, I-beam, channel steel, etc.) are made of Q235 and have a certain strength. It is suitable for engineering structures such as bridges and buildings, has good practical performance, is relatively inexpensive, and has a high cost performance ratio [6]. Q235 steel is further divided into four grades: A, B, C, and D, based on the different carbon content. The track used in this project is Q235A grade steel, with a main chemical composition of C 0,14~0,22%, Mn 0,30~0,65, Si ≤ 0,30, S ≤ 0,050, P ≤ 0,045 [7], and the remaining components are Fe. A rectangular beam with a length of 8 750 mm, a width of 550 mm, and a height of 550 mm. Pins are installed on both sides of the balance beam, and hinged plates are installed at the bottom. The assembly diagram is shown in the following Figure 1,2 and 3.

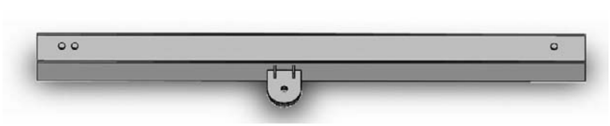

Figure 1 Three-dimensional view of assembly

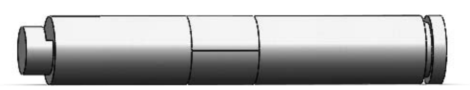

Figure 2 Three-dimensional diagram of the shaft

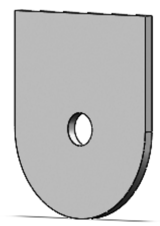

Figure 3 Three-dimensional diagram of the hinge plate

NUMERICAL SIMULATION

Firstly, use SolidWorks software to establish three-dimensional structures such as balance beams, shaft pins, hinge plates, etc., and assemble them. Convert the format and import it into Abaqus software. Perform finite element modeling on the imported assembly, observe the stress and strain situation of the balance beam, create material properties for Q235A, and assign material properties to the balance beam. Then, create an analysis step with a certain duration and frequency, select the numerical simulation data to be output, and select the stress and strain situation this time, Create interaction, set friction coefficient, and create constraints. Fix the balance axis pin to simulate the actual lifting process. Then, select the circular hole at the hinge plate as the reference point, which is coupled with the position of the hinge plate. Define boundary conditions for the reference point, restrict its movement and rotation in other directions, and set the load. Choose natural gravity 9 800 N, Then, according to the actual working conditions, calculate the force of 178 000 N that needs to be applied to the balance beam. Provide a certain initial velocity or acceleration, and the given velocity should meet the actual engineering requirements. If it is too large, it can cause safety hazards, while if it is too small, it can lead to too long the engineering time and affect efficiency. Therefore, the speed should be appropriately selected.

Grid partitioning is an important step in establishing a finite element model, which requires consideration of many issues and requires a large amount of work. The form of grid partitioning will have a direct impact on computational accuracy and scale. When dividing the grid, in order to ensure the accuracy of numerical simulation, the size of the grid should be selected according to the three-dimensional model and material properties, and should be as small as possible. The number of grids will affect the accuracy of the calculation results and the size of the calculation. Generally speaking, as the number of grids increases, the calculation accuracy will improve, but at the same time, the calculation scale will also increase. Therefore, when determining the number of grids, two factors should be considered comprehen-

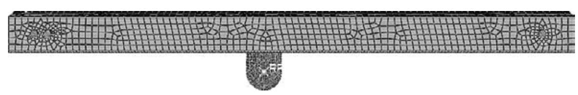

Figure 4 3D grid diagram

Table 1 **Number of grids**

Object	Volume/mm/s	Number of grids
Balancing beam	100	7 234
Pivot pin	8	13 712
Hinged plate	15	3 266

sively. Due to the fact that the balance beam, pivot pin, hinge plate and other structures are all very symmetrical and uniform in overall structure, their stress situation is relatively uniform. Therefore, when dividing the mesh, hexahedral mesh with good mesh quality is used, and corresponding mesh sizes are used according to the size of the components. This can shorten the calculation time without having a significant impact on the results. The final grid is shown in Figure 4. The specific number of grids is shown in Table 1.

Simulation results and analysis

During the lifting process of the balance beam, based on the above modeling method and the selected process parameters, finite element analysis is carried out to obtain numerical simulation results for the construction of the balance beam as a whole and its parts, Figures 5,6 and 7.

Figure 5 Stress diagram of the balance beam

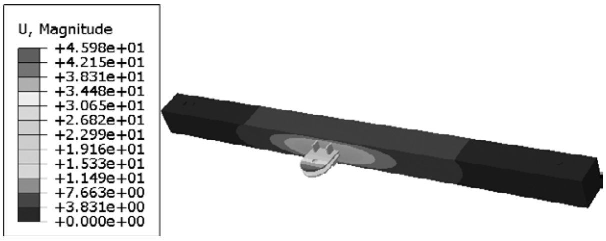

Figure 6 Strain-displacement diagram of the balance beam

Figure 7 Plastic deformation diagram of the balance beam

According to the numerical simulation results of stress-strain, it can be seen that a vertical downward tension is applied at the hinge plate to simulate the working process of the balance beam. During this process, a very large deformation is generated. However, from the stress cloud map, it can be seen that the stress at the junction plate did not reach the yield stress of Q235 at 235 MPa, and the maximum stress was 226,1 MPa. The deformation that occurred was elastic. According to the strain displacement cloud map, the maximum deformation at the hinge plate reached 45,98 mm, According to the plastic deformation Figure 7, the main location where plastic deformation occurs in the balance beam is at the contact area between the hinged plate and the beam, with the maximum plastic deformation of $3{,}629 \times 10^{-2}$ mm, the type variable is very small for the thickness of the balance beam and can be ignored.

The pivot pin of the balance beam is a fixed constraint. In the actual lifting process, it not only bears the gravity of the balance beam itself, but also bears the tension of the object on it. Therefore, numerical simulation analysis of the pivot pin should also be carried out.

Through numerical simulation cloud maps, it can be seen that significant deformation occurred at each pivot pin of the balance beam during this process. Figures

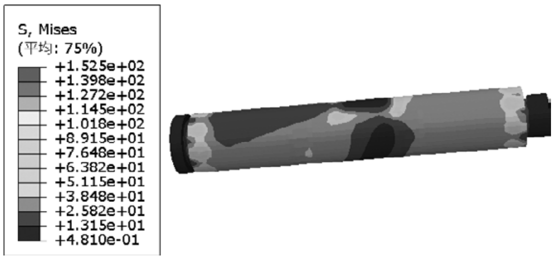

Figure 8 Stress diagram of the left pin on the balance beam

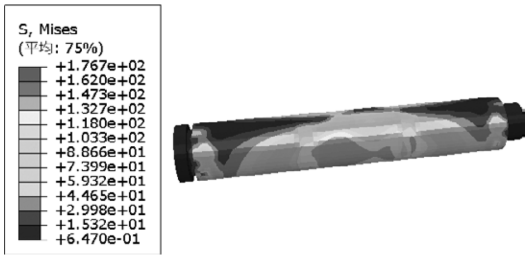

Figure 9 Stress diagram of the left second pin on the balance beam

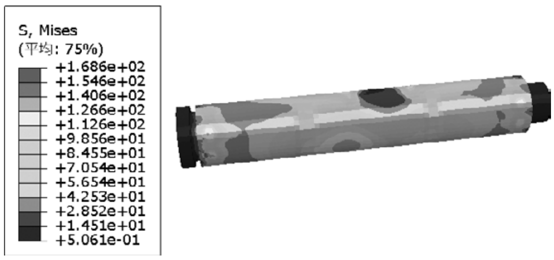

Figure 10 Stress diagram of the right pin on the balance beam

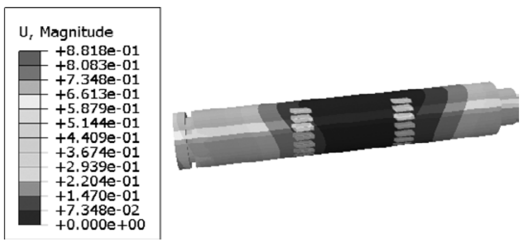

Figure 11 Elastic deformation diagram of the right pin on the balance beam

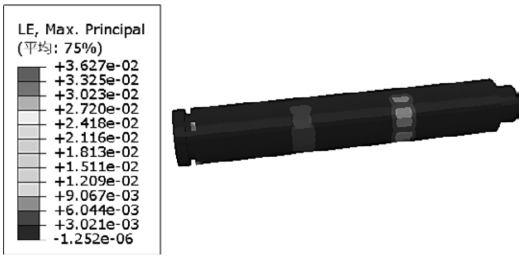

Figure 12 Plastic deformation diagram of the right pin on the balance beam

8,9,10,11 and 12. The stress on the first pivot pin on the left side of the balance beam was 152,5 MPa, the maximum stress on the second pivot pin on the left side was 176,7 MPa, and the stress on the right pivot pin was 168,6 MPa. The maximum stress on the second pivot pin on the left side did not reach the yield stress of Q235 at 235 MPa, and the deformation occurred as elastic deformation, According to the strain displacement cloud map, the maximum deformation at the pivot pin reaches 0,8818 mm, and the plastic deformation is 3,627 × 10^{-2} mm.

CONCLUSION

According to the requirements of simulating actual working conditions, adding loads and constraining them can be seen from the numerical simulation results that the maximum stress borne by the balance beam is 226,1 MPa, the maximum displacement at the hinge plate is 45,98 mm, and the maximum plastic deformation is 3,629 × 10^{-2} mm, the maximum force exerted on the three shaft pins is 176,7 MPa, the maximum deformation reaches 0,8818 mm, and the maximum plastic deformation is 3,627 × 10^{-2} mm. The stress borne did not reach the yield stress of Q235 at 235 MPa, which is within the allowable range and meets the requirements of the working conditions.

Acknowledgments

This work is supported by China Minmetals Group Co., Ltd. Science and Technology Special Plan Project (2021ZXA06) and funded by Science Research Project of Hebei Education Department (CXY2024054).

REFERENCES

[1] M Ghafouri, J Ahn, J Mourujärvi, et al. Finite element simulation of welding distortions in ultra-high strength steel S960 MC including comprehensive thermal and solid-state phase transformation models[J]. Engineering Structures, (219)2020, 110804.

[2] J Bonilla, E Mirambell, et al. Numerical analysis of curved steel plate girders subjected to patch loading[J]. Engineering Structures, (297)2023, 117015.

[3] Q. Y. Xu, H. Sun. et al. Analysis of ultimate seismic performance of thin-walled concrete-filled steel tube bridge piers under dynamic load[J]. Engineering Structures, (292)2023, 116544.

[4] H. Zhao, R. Wang. et al. Experimental and numerical investigation on impact and post-impact behaviours of H-shaped steel members[J]. (216)2020, 110750.

[5] Q. Lu, X. L. Deng. Energy absorption and in-plane mechanical behavior of honeycomb structures with reinforced strut[J]. 322)2023, 117399.

[6] X. A. Zha. High Entropy Welding of 304/Q235 Stainless Steel Composite Plate [D]. East China Jiaotong University,2022.

[7] Y. P. Tian. Preparation and Properties of Wear Resistant Coating on Q235 Steel Surface [D]. Changzhou University,2022.

Note: The responsible translator for English language is W LIU-North China University of Science and Technology, China